Effect of Thermal Aging on the Interfacial Reactions of Tin-Based Solder Alloys and Copper Substrates and Kinetics of Formation and Growth of Intermetallic Compounds

(Efeito do envelhecimento térmico nas reações interfaciais de ligas de soldagem branda a base de estanho em substratos de cobre e cinética de formação e crescimento de compostos intermetálicos)

J. C. Madeni and S. Liu
Center for Welding, Joining and Coatings Research, Metallurgical & Materials Engineering Department, Colorado
School of Mines, U.S.A., sliu@edu.mines

ABSTRACT

The formation and growth of intermetallic compounds at the interface between four solder alloys, Sn-3.5Ag, Sn-0.7Cu, Sn-3.2Ag-0.8Cu and Sn-9Zn, and Cu-plated substrates have been studied. Thermal aging tests for 20, 100, 200, 500 hours at 70, 100 and 150 ºC were carried out. As expected, results indicate that the formation of the intermetallic layer is a diffusion-controlled process. Nevertheless, migration and dissolution of Cu into the solder was observed, especially at lower temperatures. The thickness of the layer of intermetallic compound increased with increasing aging temperature and time. The Sn-3.5Ag alloy showed the smallest intermetallic growth and the Sn-9Zn alloy the highest, compared to the other alloys. The results also show definite morphological differences between the Cu/Cu$_3$Sn, the Cu$_3$Sn/Cu$_6$Sn$_5$ and the Cu$_6$Sn$_5$/solder-matrix interfaces.

Key Words: *Tin-based solder alloys, Intermetallic compounds, Isothermal aging, Morphology, Interface, IMC layer growth front.*

Resumo*: A formação e o crescimento de compostos intermetálicos na interface entre quatro ligas de soldagem branda, Sn-3.5Ag, Sn-0.7Cu, Sn-3.2Ag-0.8Cu e Sn-9Zn e substratos revestidos com Cobre foram estudados. Testes de envelhecimento térmico de 20, 100, 200, 500 horas a 70, 100 e 150 ºC, foram realizados. Como esperado, os resultados indicam que a formação da camada de intermetálicos é um processo controlado por difusão. No entanto, a migração e dissolução de Cu na solda foi observado, especialmente em baixas temperaturas. A espessura da camada de compostos intermetálicos aumentou com o aumento da temperatura e do tempo de envelhecimento. A liga de Sn-3.5Ag apresentou o menor crescimento de intermetálicos e a Sn-9Zn o mais elevado, comparado com as outras ligas. Os resultados também mostram diferenças morfológicas entre as interfaces Cu/Cu$_3$Sn, Cu$_3$Sn/Cu$_6$Sn$_5$ e Cu$_6$Sn$_5$.*

Palavras chave: *Ligas para soldagem branda a base de estanho, Compostos intermetálicos, Envelhecimento isotérmico, Morfologia, Interface, Frente de crescimento de camada IMC.*

1. Introduction

Health and environmental concerns in the electronic packaging industry regarding the use of lead-based alloys led to the search for lead-free substitute alloys. Previous studies have shown that Sn-based alloys such as Sn-3.5Ag, Sn-0.7Cu, Sn-3.2Ag-0.8Cu and Sn-9Zn exhibit promising mechanical properties [1-3] and can be considered as serious candidates to replace the Sn-Pb alloy. Nevertheless, more information is needed before life and reliability predictions can be made for joints using these materials. During reflow soldering, a layer of intermetallic compound (IMC) is formed between the substrate and the solder alloy. In solid-state this layer continues to grow and may react to produce additional IMC layers [4]. The concern about these IMCs is that at high operating temperatures they may grow to become detrimental to the mechanical integrity of the solder joints [3,5]. This study provides information about the effects of annealing on the solder/substrate interface morphology and microstructure. For that purpose, the formation and growth of intermetallic layers between the copper-plated substrates and the Sn-3.5Ag, Sn-0.7Cu, Sn-3.2Ag-0.8Cu and Sn-9Zn alloys is investigated.

2. Experimental Procedure

2.1. Production of copper/solder joints

The melting temperatures of the solder alloys utilized in this study are shown in Table 1. The number in front of each element symbol represents its weight percent in the alloy. For example, there is 0.7 wt. pct. of copper in Sn-0.7Cu alloy. The substrate was a commercial Cu-plated printed circuit board (PCB). The PCB board was cut in pieces of 25.4 x 25.4 mm (1 x 1 inch). Prior to producing the joints, the Cu substrates were cleaned with a water-based solution of ammonium hydroxide, trisodium phosphate and sodium tetraborate pentahydrate (also known as M-prep neutralizer). For Sn-3.5Ag, Sn-0.7Cu and Sn-3.2Ag-0.8Cu alloys, after letting the copper surface dry for a few seconds, a solution of water-based phosphoric acid (M-prep conditioner) was applied. These solutions removed

86

Soldag. insp. São Paulo, Vol. 16, No. 1, p.086-095, Jan/Mar 2011

any impurities, dirt, and oxide layers present on the surface and promoted wetting. In the case of the Sn-9Zn alloy, a commercial zinc chloride and ammonium chloride based paste was applied to the copper surface, which provided better wetting than the phosphoric acid-based solution applied to the copper substrate for the three previous solder alloys. The solder drops were melted on the substrate at a temperature 50°C above their respective melting temperatures indicated in Table 1, under argon gas. The joints, with approximately 3mm thick solder, were cooled in air to room temperature.

Table 1. Melting and furnace temperatures for the solder alloys used in this study.

Solder alloy	Melting Temperature, (°C)	Furnace Temperature ± 1°C, (°C)
Sn-3.2Ag-0.8Cu	217	267
Sn-3.5Ag	221	271
Sn-0.7Cu	227	277
Sn-9Zn	198.5	248

2.2. Thermal aging test

The thermal aging tests of the copper/solder joint coupons were done using furnaces with temperatures controlled to ± 1°C. To avoid oxidation during thermal aging, a continuous flow of industrial grade argon gas was provided to the furnaces. The copper/solder joints were thermally aged at 70, 100 and 150 °C, and for 20, 100, 200 and 500 hours. The specimens were water-quenched as they were removed from the furnaces.

2.3. Interface characterization

Each sample was cut in half and cold mounted using epoxy for metallographic analysis. The reason for using cold mounting instead of hot mounting is that cold mounting undergoes a lower curing temperature. The mounted samples were ground and polished using standard metallographic techniques, first to 0.5 mm with diamond slurry, and then to 0.05 mm for 45 minutes using colloidal silica. Polishing the samples in a vibratory machine with colloidal silica resulted in a good etched surface.

The samples were analyzed using light microscopy and scanning electron microscopy (SEM) to characterize the different microstructural features and energy dispersive spectroscopy (EDS) to identify the intermetallic compounds. Quantification of IMC thickness was done by measuring the linear distance from the edge of the copper substrate to the IMC layer growth front. In the same manner, the measurement of the average total IMC layer thickness when two layers were present was done measuring the linear distance from the edge of the copper substrate to the second IMC layer growth front. Eighty thickness readings along the interface at consistent intervals were averaged

to obtain the average IMC layer thickness for each of the solder alloy-substrate combinations. The IMC thickness measurements were performed using the image analysis software incorporated in the scanning electron microscope.

3. Results And Discussion

3.1. Joint interface characterization

Micrographs of the Cu/Solder alloy interface after soldering, such as the one in Figure 1, indicate the existence of a very small Cu_6Sn_5 intermetallic layer visible only at high magnifications [5, 6]. In the tin/copper and tin-rich-alloys/copper joint systems, the intermetallic Cu_6Sn_5 (h'-phase) formed immediately upon contact of the liquid solder with the copper substrate [7, 8]. Then, the intermetallic compound grew rapidly [9,10].

Figure 1. Micrograph of the Cu/Sn-3.5Ag interface after soldering, showing the presence of the Cu_6Sn_5 intermetallic layer.

The interface after thermal aging was found to be very different compared to the initial observations immediately following soldering, as shown in Figure 2, in the micrographs of the Cu/Solder interface at 150 °C for 500 hours. Beginning from the bottom, in Figures 2(a), (b) and (c), the visible layers are the epoxy board, the copper substrate, the intermetallic compounds (IMCs), Cu_3Sn and Cu_6Sn_5, and finally the solder matrix. It was observed that the layer of Cu_3Sn formed at the Cu/solder interface when the joint was under thermal aging, and the layer of Cu_6Sn_5 resulted on top of Cu_3Sn. This sequence is true for the three solder alloy systems, Cu/Sn-3.2Ag-0.8Cu, Cu/Sn-3.5Ag, and Cu/Sn-0.7Cu. In the case of Cu/Sn-3.5Ag, a few small particles of Ag_3Sn can also be observed along the Cu_6Sn_5/Sn-3.5Ag interface. Different from the previous joint systems, the Cu/Sn-9Zn system displayed only one intermetallic layer, Cu_5Zn_8 as evidenced in Figure 2(d).

3.2. Identification of the intermetallic compounds

Energy dispersive spectroscopy (EDS) analysis was used to identify the intermetallic compounds present in each of the joint samples. The characteristic x-ray intensity spectrum and the chemical data Sn = 46.33 at. pct. and Cu = 53.67 at. pct. (close to the 6:5 Cu/Sn molar ratio) in Figure 3(a) clearly show intensity peaks corresponding to the h'-phase in the copper-tin phase diagram (included as Appendix A), which is the Cu_6Sn_5 intermetallic compound. This IMC is present in the as-soldered and annealed samples.

Similarly the data in Figure 3(b) was analyzed. The high Cu and lower Sn x-ray intensity peaks indicate that copper is the major component of the compound. The chemical composition, Sn = 24.35 at. pct. and Cu = 75.65 at. pct., which is close to the 3:1 molar ratio of Cu/Sn, approaches the stoichiometric composition of Cu_3Sn. Using the atomic percent of the two elements given above on the copper-tin phase diagram in

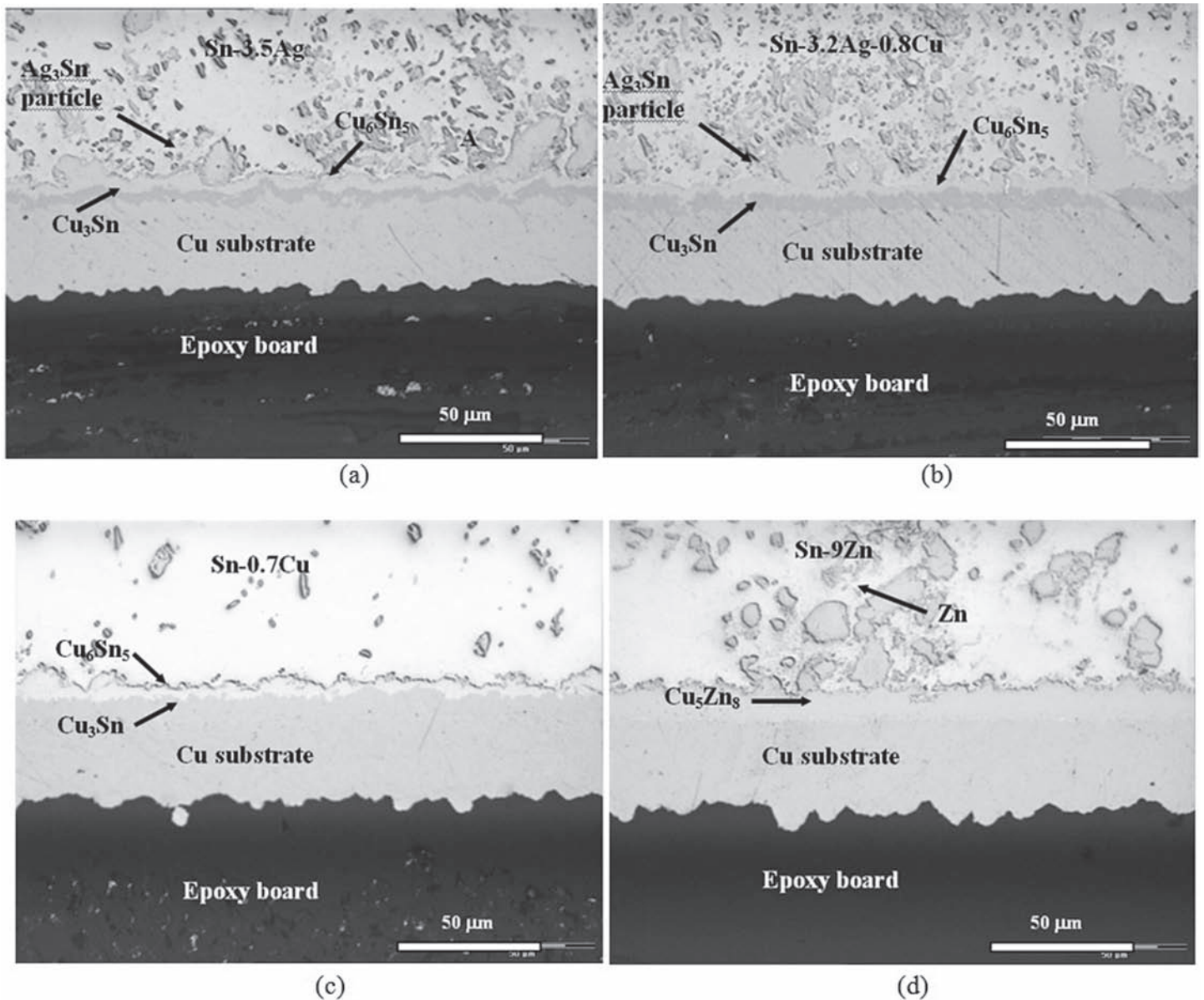Soldag. insp. São Paulo, Vol. 16, No. 1, p.086-095, Jan/Mar 2011

87

Figure 2. Micrographs of the Cu/solder interfaces at 150°C for 500 hours, for the four solder alloy systems, indicating their respective intermetallic layers, (a) Cu/Sn-3.5Ag, (b) Cu/Sn-3.8Ag-0.8Cu, (c) Cu/Sn-0.7Cu, and (d) Cu/Sn-9Zn.

Appendix A, the compound falls inside the e-phase region, which indeed is the Cu_3Sn intermetallic. The EDS spectrum in Figure 3(c) was obtained from area "A" in the micrograph in Figure 2(a), which indicates higher number of counts (peaks) of silver compared to those of tin. The data points indicate Sn and Ag in the amounts of 24.77 at. pct. and 75.23 at. pct., respectively. Locating these atomic percents on the tin-silver phase diagram in Appendix B, the intermetallic compound can be determined as Ag_3Sn (g-phase).

The EDS spectrum in Figure 3(d) indicates the presence of two elements, copper and zinc; the larger number of zinc peaks suggest higher amounts of zinc. Indeed, the atomic percent of copper and zinc, 35.10 at. pct. and 64.90 at. pct., respectively, confirm the existence of more zinc in the compound. Locating these amounts of copper and zinc on the copper-zinc phase diagram shown in Appendix C, it is found that the intermetallic is the Cu_5Zn_8 (g-phase). The intermetallic compounds identified in this study are in agreement with previous reports made by J.Y. Park et al. [11], and C. Hang et al. [12].

3.3. Morphology of the intermetallic layers

Evidence of interface morphological differences was found between the IMCs. The Cu_3Sn/Cu_6Sn_5 interface was observed to be irregular [11-13]. The thickness variation of the Cu_3Sn intermetallic layer was not as drastic as the thickness of the Cu_6Sn_5 intermetallic layer. In the case of the Cu_6Sn_5/solder-matrix, the interface is more irregular, with localized developments of elongated, needle-like, or elongated scalloped structures [14,15], growing far into the solder matrix. According
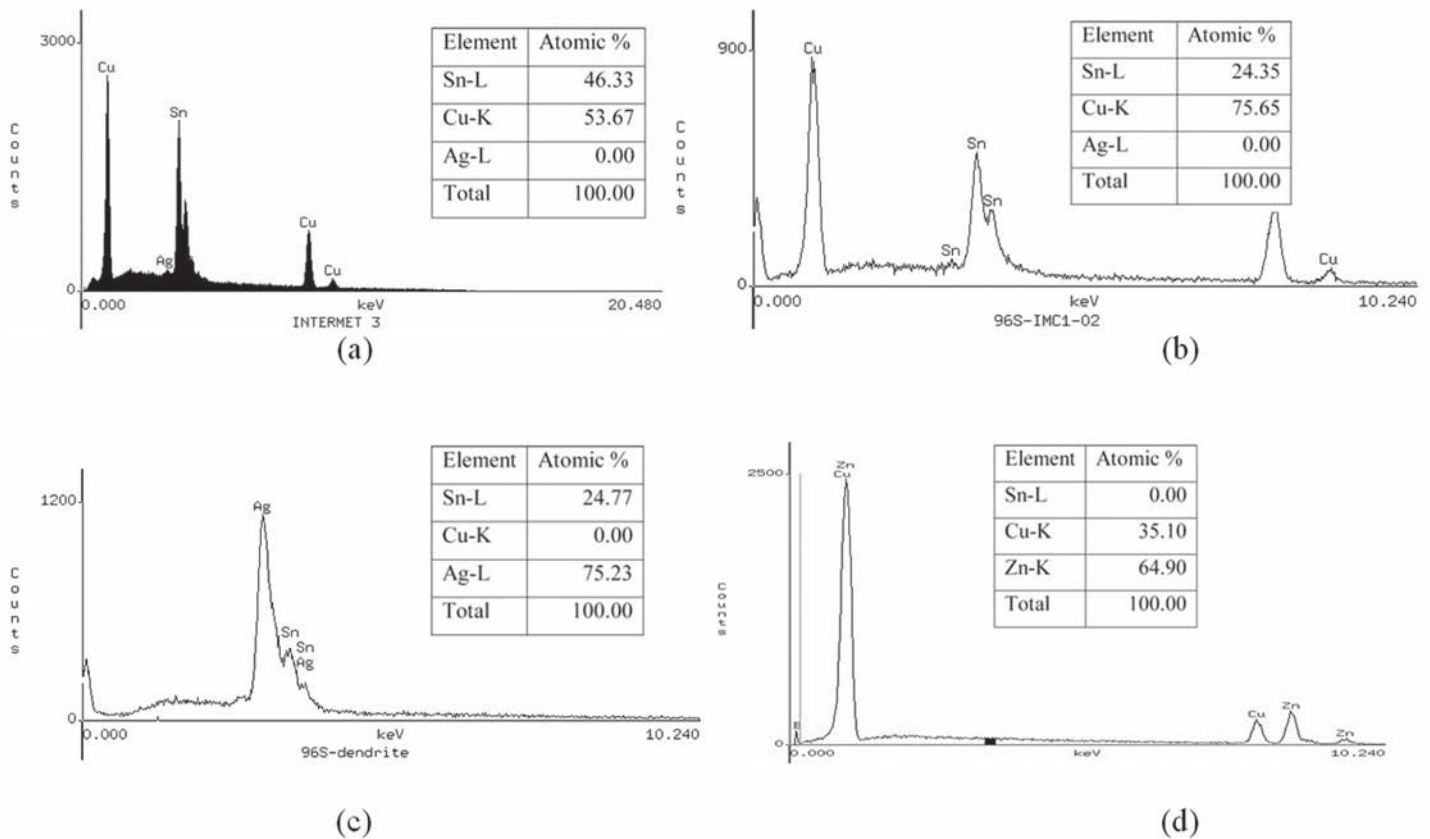
Figure 3. EDS spectrum identifying the intermetallic compounds at the Cu/solder interface. (a) Cu_6Sn_5, (b) Cu_3Sn, (c) Ag_3Sn, (d) Cu_5Zn_8.

to Y.G. Lee et al. [6] the irregularity of the solder/IMC interface takes place during a liquid-solid reaction during soldering.

Cu/Sn-3.5Ag System

In the case of the Cu/Sn-3.5Ag system, the morphology of the Cu_6Sn_5 layer is significantly different from that of Cu_3Sn. Figure 4(a) clearly exhibits the irregular interface of the Cu_6Sn_5 intermetallic, protruding into the solder matrix. Some areas of this interface (growth front) developed into elongated, needle-like morphologies such as the one shown in the micrograph. In other areas, the initiation of the needle-like morphologies, "A", and the formation of the scalloped structures [16], "B", were observed, Figure 4(a). In addition, Ag_3Sn was found in the form of small particles at the Cu_6Sn_5/solder interface. It is plausible that these small particles of Ag_3Sn interrupted the fast growth of the Cu_6Sn_5 layer. The growth front of the Cu_3Sn layer is not as irregular as that of the Cu_6Sn_5. For better visual clarification of the micrograph in Figure 4(a), the Cu_3Sn growth front has been outlined with a dash-dotted line, and the copper surface with a dashed line. It seems that the irregularity of the Cu_3Sn layer depended more on the original surface of the copper substrate.

Cu/Sn-3.2Ag-0.8Cu System and Cu/Sn-0.7Cu System

In the case of the Cu/Sn-3.2Ag-0.8Cu and Cu/Sn-0.7Cu, the interface of the Cu_6Sn_5 is smoother than that observed in the Cu/

Sn-3.5Ag system. Evidence of this observation can be found in Figures 4(b) and (c). Figure 4(b) displays the Cu/Sn-3.2Ag-0.8Cu interface. The most noticeable feature of this interface is that the Cu_6Sn_5 growth front was irregular but did not have sharp features as in the previous case of Cu/Sn-3.5Ag. For example, the needle-like and scalloped structures are not present here. The Cu_3Sn growth front was also irregular.

In the case of the Cu/Sn-0.7Cu interface shown in Figure 4(c), the irregularity of the Cu_6Sn_5 growth front was more than in the case of the Cu/Sn-3.2Ag-0.8Cu. This interface also exhibited small pieces of Cu_6Sn_5 (~1 to 2 microns in size) detached from the Cu_6Sn_5 layer, but they did not seem to grow far into the solder matrix. Again, the Cu_3Sn growth front exhibited irregular characteristics.

Cu/Sn-9Zn System

The most significant difference between the Cu/Sn-9Zn interface and the interfaces of the other three systems is that the Cu/Sn-9Zn interface exhibited only one intermetallic layer, which was identified as Cu_2Zn_8. The growth front of this layer, as seen in Figure 4(d), was irregular, finely jagged, but did not present sharp irregularities as in the case of the Cu/Sn-3.5Ag.
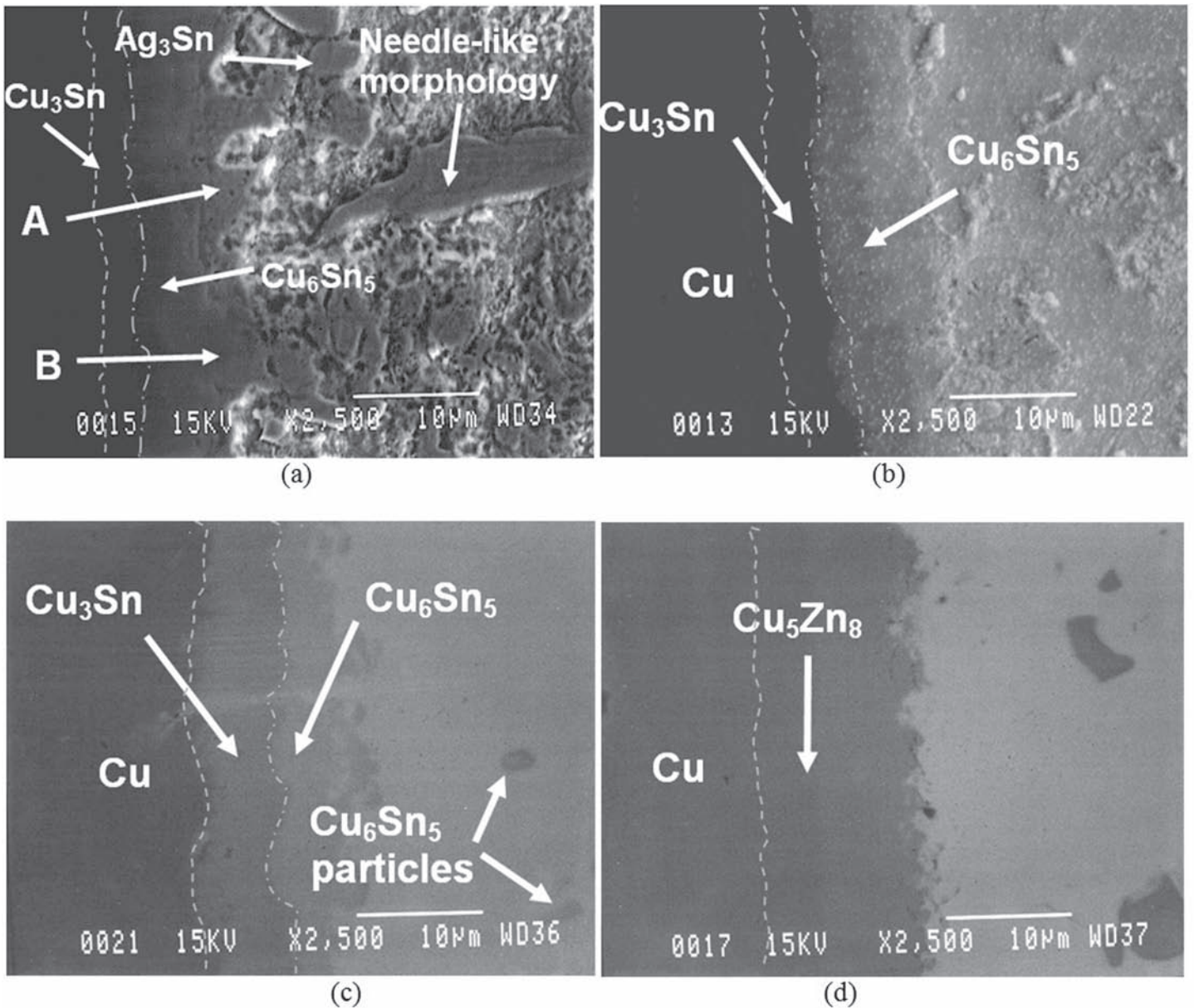
Soldag. insp. São Paulo, Vol. 16, No. 1, p.086-095, Jan/Mar 2011

89

Figure 4 (a) Cu/Sn-3.5Ag interface exhibiting the irregularity of the Cu_3Sn and Cu_6Sn_5 intermetallics growth front and the Ag_3Sn scalloped and needle-like morphologies. (b) Secondary electron image of the Cu/Sn-3.2Ag-0.8Cu interface, and (c) Backscattered electron image of the Cu/Sn-0.7Cu interface, and (d) Backscattered electron image of the Cu/Sn-9Zn interface.

3.4. Kinetics of intermetallic layer growth

The growth kinetics of the IMCs as a function of aging time and temperature was analyzed by evaluating the thicknesses of the IMC layers. The method of determining the IMC thickness was presented in the experimental section of this document. The thicknesses of individual Cu_3Sn and Cu_6Sn_5 layers and combined (Cu_3Sn + Cu_6Sn_5) IMC layers were measured. The total intermetallic layer thickness measured in the four material systems at 150°C, the highest aging temperature used in the experiments, and for 500 hours were determined in the following: 13.3 mm for Cu/Sn-3.5Ag, 13.6 mm for Cu/Sn-3.2Ag-0.8Cu, 14.1 mm for Cu/Sn-0.7 Cu, and 19.1 mm for the Cu/Sn-9Zn alloy.

A simple parabolic, diffusion-controlled growth model, represented by equation (1), was assumed in the analysis of these experiments.

$$X = (kt)^{1/2} \qquad (1)$$

X is the thickness of the intermetallic layer, k is the growth constant, and t the time. The observed total IMC thickness and time relationships at 70, 100 and 150 °C, shown in Figures 5(a), (b) and (c) respectively, were found to obey the parabolic relationship assumed previously. Other researchers such as Vianco et al.[17] and Lee et al.[6] have found similar relationships. The slopes of the lines in Figure 5 indicate the rate of IMC
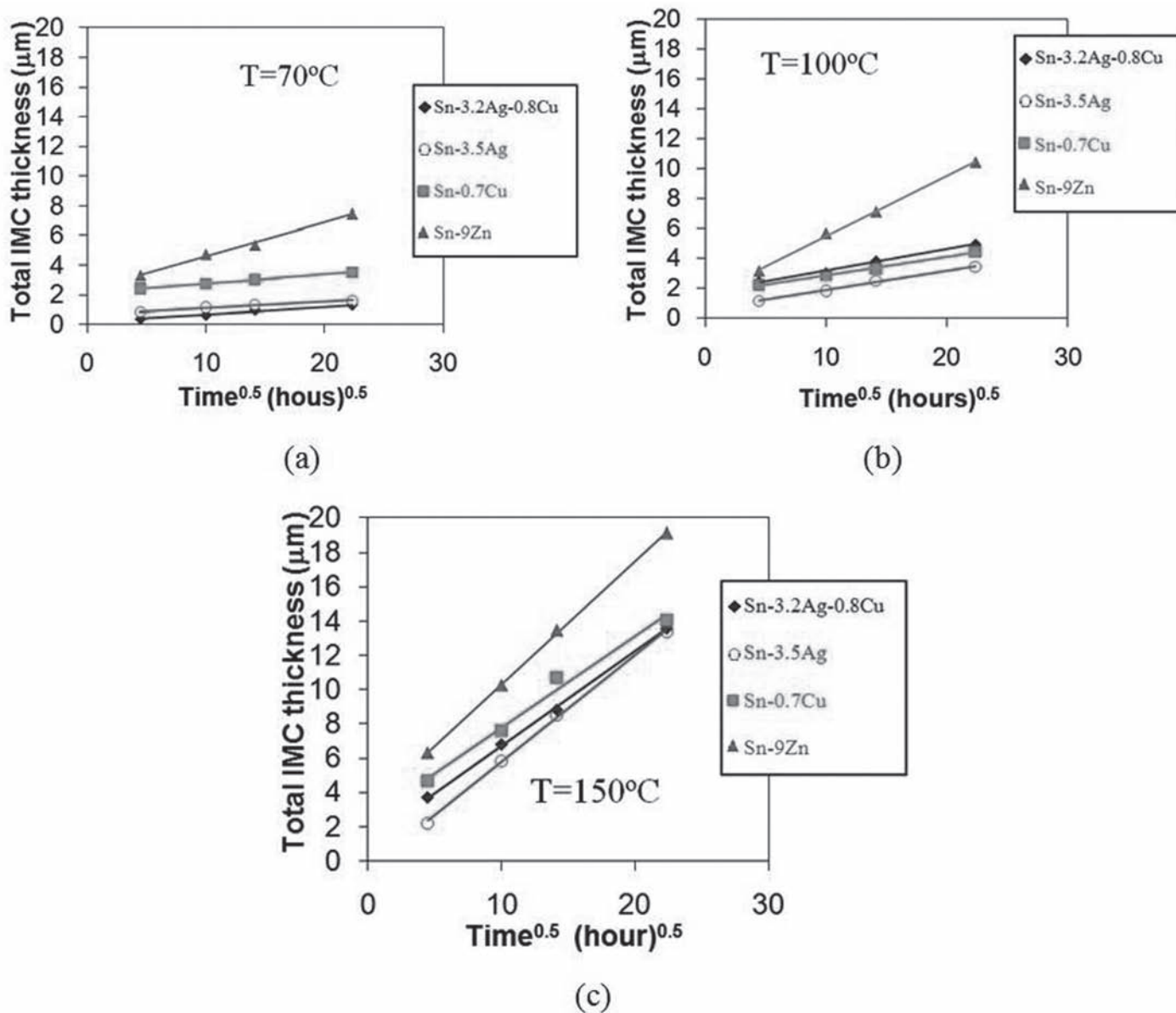
90

Soldag. insp. São Paulo, Vol. 16, No. 1, p.086-095, Jan/Mar 2011

Figure 5. Total IMC growth ($Cu_3Sn + Cu_6Sn_5$) at the Cu/solder interface at three temperatures, (a) 70 ᵒC, (b) 100 ᵒC, and (c) 150 ᵒC.

growth; therefore, as the temperature increased, the rate of IMC layer growth increased. At the three temperatures, the Sn-9Zn alloy grew at the fastest rate. The Sn-3.5Ag alloy grew at the slowest rate at 70 and 100 ᵒC, and the Sn-3.2Ag-0.8Cu alloy at 150 ᵒC.

Similar analysis was conducted for each of the individual IMCs in each Cu/solder system. The general observation is that their growth also obeyed the parabolic growth as in the case of the growth of the total IMC. Figure 6 shows how the individual IMCs grew with time.

In the case of the Cu/Sn-3.2Ag-0.8Cu joint system, shown in Figure 6(a), the growth rate of the two intermetallic compounds, Cu_6Sn_5 and Cu_3Sn, are statistically similar. In the case of the Cu/Sn-3.5Ag system, shown in Figure 6(b), the Cu_6Sn_5 layer grew at a faster rate than the Cu_3Sn layer. This observed trend can be explained as since abundant tin atoms are available they

first react with the available copper atoms at the site and form Cu_6Sn_5. Cu_3Sn did not grow as fast as in the previous case because less Sn atoms were available to react with Cu atoms, since Sn would be reacting with Ag to form Ag_3Sn at the Cu_6Sn_5 growth front. The remaining tin atoms at the Cu_6Sn_5/solder interface would enhance the diffusion of tin through the Cu_6Sn_5 intermetallic layer to react with the copper atoms to form the Cu_3Sn intermetallic.

In the case of the Cu/Sn-0.7Cu system shown in Figure 6(c), larger amounts of Cu_3Sn formed but grew at approximately the same rate than Cu_6Sn_5. The Cu_3Sn layer grew because no Ag_3Sn were formed in this system. Therefore, more tin atoms would take part in the diffusion of tin though the Cu_6Sn_5 layer to form Cu_3Sn. In the case of the Cu/Sn-9Zn system, only Cu_5Zn_8 formed. Therefore, Cu_5Zn_8 is considered as the total IMC layer. The results obtained in this study indicate that the IMCs were
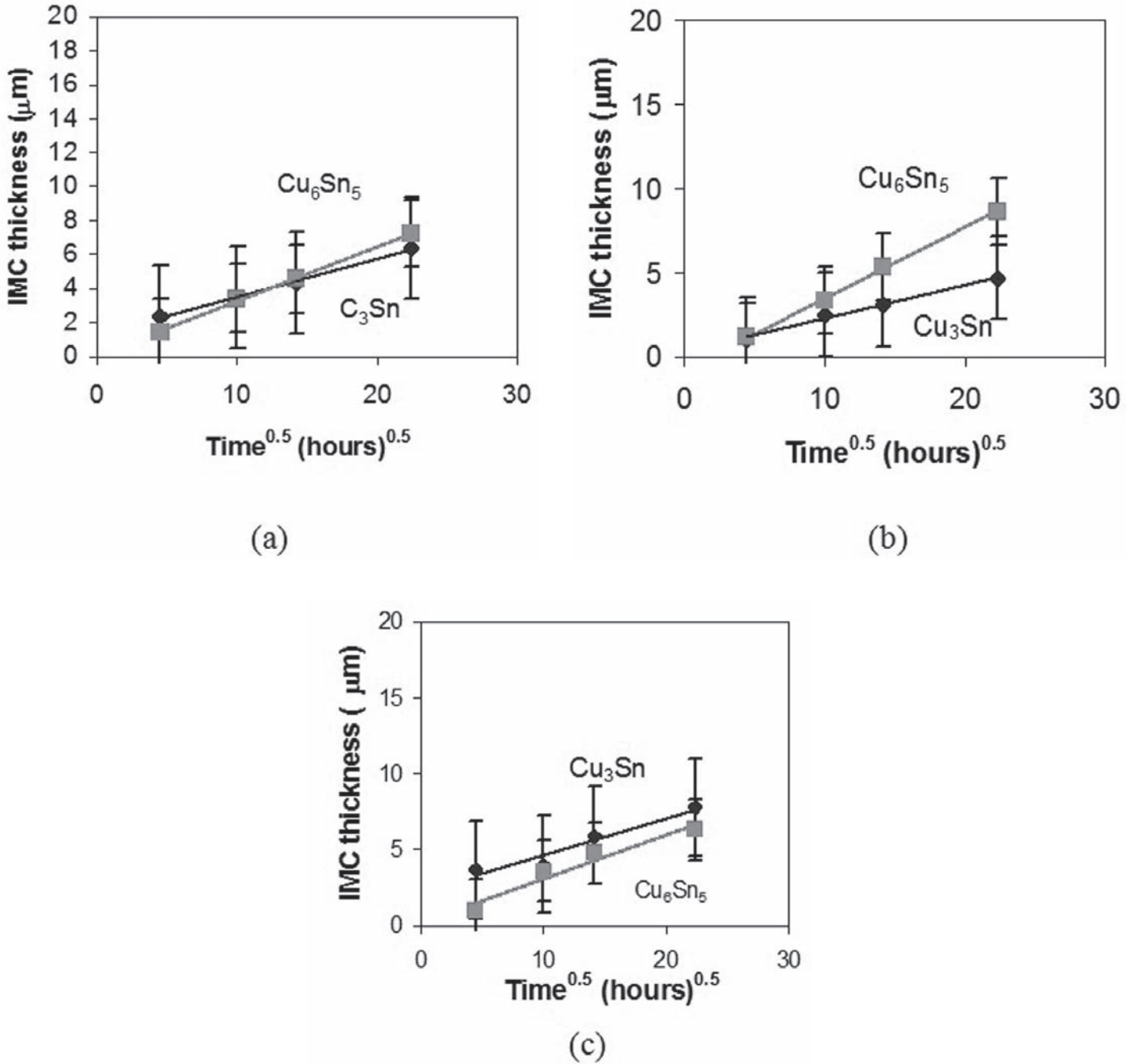
Figure 6. Individual IMC layers growth for samples aged at 150 ºC, (a) Cu/Sn-3.2Ag-0.8Cu, (b) Cu/Sn-3.5Ag, and (c) Cu/Sn-0.7Cu.

formed by the reaction of tin and copper atoms at the solder/substrate interface and by the diffusion of copper and/or tin atoms through the layer. This IMC process formation is discussed by Vianco et al. [17]. The theory indicated by Flanders et al.[6], states that tin atoms travel towards the copper substrate, first to form Cu_6Sn_5 and then through the Cu_6Sn_5 layer to form Cu_3Sn. However, if that would be the case, the activation energy for the formation of Cu_6Sn_5 would have been lower but it is not, as is shown in Table 2. It should be noted that at lower activation energies the reaction would proceed easier than at higher

activation energies. According to Y.G. Lee et al.[6] and D. Yao et al. [18] there are also different mass transport processes that occur at the solder/substrate interface, such as channels between grains serving as fast diffusion and dissolution paths of Cu in the solder to feed the reaction. However, they also recognize that during aging bulk diffusion is the dominant mechanism of mass transport for the growth of intermetallic compounds. Strong evidence of copper diffusion through the Cu_6Sn_5 layer to react with Sn-3.5Ag was reported by S.J Wang et al. [19]. For detailed description the reader is referred to reference 19.

92

Soldag. insp. São Paulo, Vol. 16, No. 1, p.086-095, Jan/Mar 2011

Table 2. Activation energy data for the Cu/Sn-3.5Ag and Cu/100Sn solder systems found in the literature compared to the data for the Cu/Sn-3.5Ag in this work.

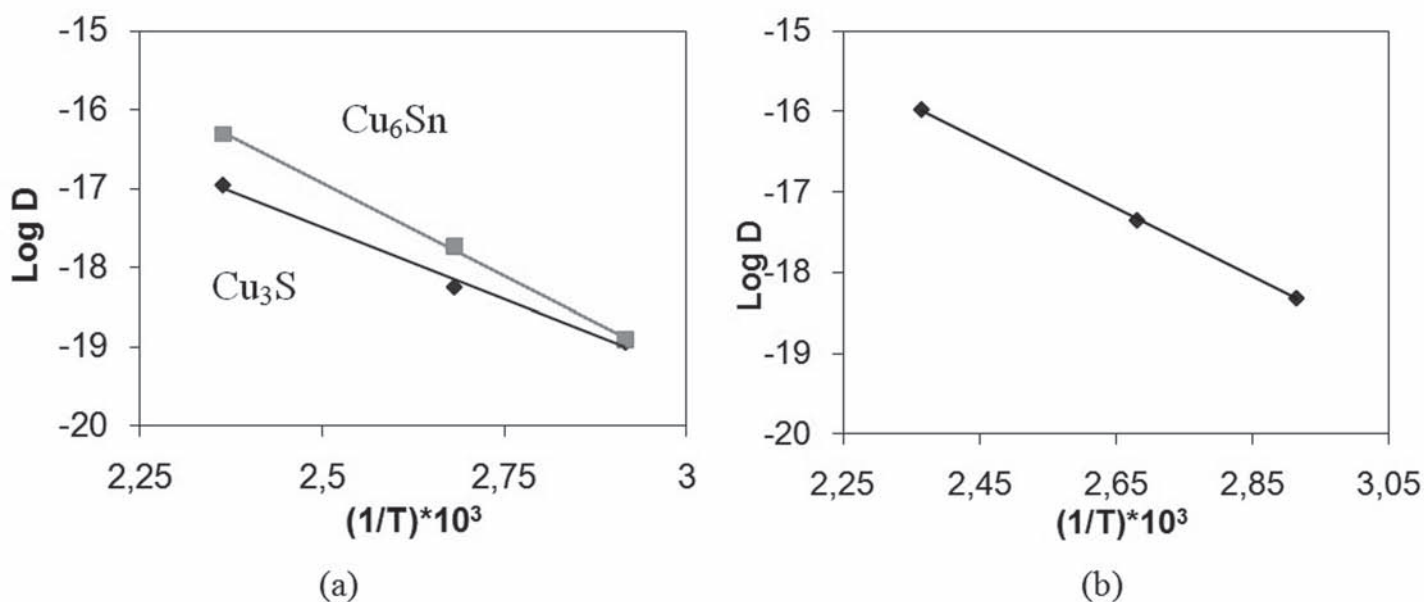| Joint	Q (eV/atom)		Total Q	Reference
System	Cu_3Sn	Cu_6Sn_5	(eV/atom)	
Cu/Sn-3.5Ag	---	1.20	1.20	Choi et al.[22]
	0.73	1.11	---	Flanders et al.[13]
	0.72	0.93	0.85	This work
	---	---	0.80	Harris et al.[5]
	---	---	0.67	Lee et al.[23]
	0.52	---	0.61	Vianco et al.[17]
Cu/100Sn	0.74	0.83	---	Vianco et al.[20]

Figure 7. Experimental data for the Cu/Sn-3.5Ag system, (a) diffusion data for the individual Cu_3Sn and Cu_6Sn_5 IMCs plotted to determine the activation energy Q, and (b) diffusion data for the combined IMC ($Cu_3Sn + Cu_6Sn_5$) plotted to determine the activation energy Q, for the combined IMC growth.

The constant k in Equation (1) was determined from the slopes of the lines in the IMC thickness versus time$^{0.5}$ plots, Figure 5. Using the Arrhenius equation below,

$$k = ko \exp\left(\frac{-Q}{RT}\right) \quad (2)$$

where k_o is the pre-exponential term, Q the activation energy, R the Universal Gas Constant and T, the absolute temperature. The log k versus $(1/T)$ plots for the individual phases and for the total IMC can be made. Both Figures 7(a) and (b) are for the Cu/Sn-3.5Ag system. The slopes of the lines in Figure 7(a) suggest higher activation energy for Cu_6Sn_5 formation than for Cu_3Sn. The line in Figure 7(b) corresponds to the combination of the two intermetallic phases in one layer. As expected, its slope suggests intermediate activation energy value.

The activation energies, Q, were calculated from the slope of the Arrhenius plot using a linear regression model. As the activation energy of a specific intermetallic compound increases, the formation and growth of this compound is expected to be more difficult. On the other hand, low activation energies indicate easier IMC formation and growth. The results of the activation energies for the total IMC thickness and for the individual phases for the four solder alloys are presented in Table 3. The activation energy data for the Cu/Sn-3.5Ag and Cu/Sn-0.7Cu joint systems are in good agreement with previous studies found in the literature [3,8]. In the case of the Cu/Sn-3.2Ag-0.8Cu and Cu/Sn-9Zn joint systems, no comparison data were found in the literature.

Table 3. Activation energies, Q, determined experimentally for the total (combined) and individual IMCs in the Cu/Sn-3.8Ag-0.8Cu, Cu/Sn-3.5Ag, Cu/Sn-0.7Cu, and Cu/Sn-9Zn joint systems.

ALLOY	IMC	Q (kJ/mol)	Q (eV/atom)
Sn-3.2Ag-0.8Cu	Total	70.9	0.74
	Cu_3Sn	69.2	0.72
	Cu_6Sn_5	72.2	0.75
Sn-3.5Ag	Total	81.6	0.85
	Cu_3Sn	69.2	0.72
	Cu_6Sn_5	90.0	0.93
Sn-0.7Cu	Total	65.5	0.68
	Cu_3Sn	59.2	0.61
	Cu_6Sn_5	72.2	0.75
Sn-9Zn	Cu_5Zn_8	33.8	0.35

As discussed earlier, data for the Cu/Sn-3.5Ag were collected from the literature [18,20-24] and reported in Table 2. Data obtained in this work were also included in the table for comparison. In this work the activation energies determined for the individual intermetallic compounds, Cu_3Sn and Cu_6Sn_5, are 0.72 and 0.93 eV/atom, respectively. Table 3 shows that Flanders et al. have obtained almost similar activation energy for Cu_3Sn (0.73 eV/atom) and much higher for Cu_6Sn_5 (1.11 eV/atom). The value of 0.8 eV/atom for the total activation energy reported by Harris agrees with the 0.85 eV/atom obtained in this work. Nevertheless, the values reported by Vianco et al. of 0.52 eV/atom for the Cu_3Sn IMC and 0.61 eV/atom for the total IMC are lower than all the data in table 3. This difference may be due to the different processes utilized in the production of the joint specimens. It is shown by Lee et al.[6] that furnace heating soldering process would produce higher amounts of IMCs than hot dipped and electroplating, in that order. Vianco [20] reported the behavior of IMCs in Sn-rich solder alloys in an electronic joint. Table 3 shows that the activation energies for this system are 0.74 eV/atom for the Cu_3Sn IMC and 0.83 eV/atom for the Cu_6Sn_5 IMC. These data is in close agreement with the data obtained in this work.

4. CONCLUSIONS

Two intermetallic compounds Cu_3Sn and Cu_6Sn_5 form at the Cu/Sn-3.5Ag, Cu/Sn-3.2Ag-0.8Cu, and Cu/Sn-0.7 Cu interfaces. In the case of the Cu/Sn-9Zn system, the IMC is Cu_5Zn_8. The three intermetallic layers grew by thermal activation in a parabolic manner. If IMC formation were the sole criterion for determination of candidates for replacing the Sn-Pb alloys, the ranking would be: Sn-3.5Ag, Sn-3.2Ag-0.8Cu, Sn-0.7Cu and Sn-9Zn, being Sn-3.5Ag the system that exhibited the least IMC growth. The Sn-3.5Ag system also reported the highest activation energy to promote combined IMC formation, 0.85 eV/atom.
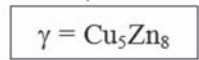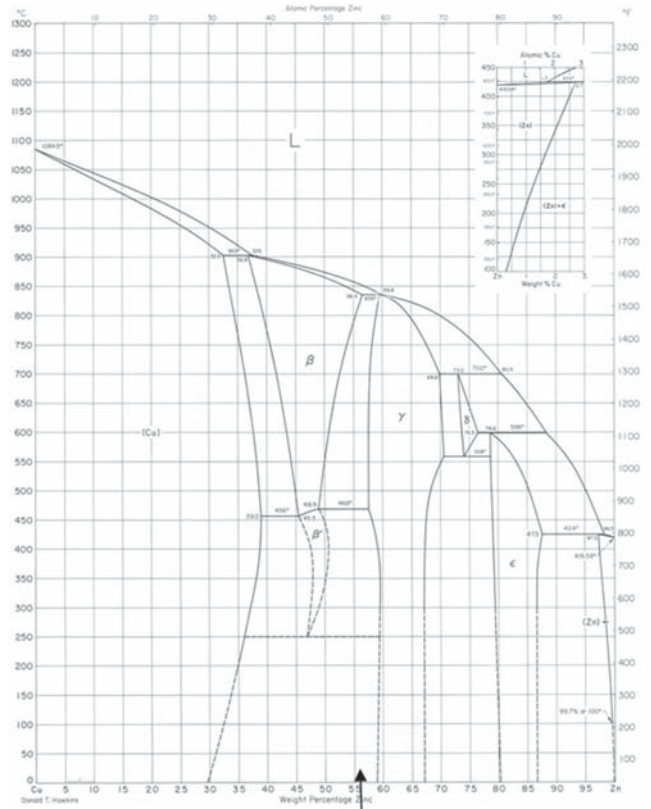
5. ACKNOWLEDGEMENTS

6. REFERENCES

[1] N.C. Lee, *Soldering Surf. Mount Technol.* 26, 65 (1997)

[2] M. Abtew and G. Selvaduray, *Mater. Sci. Eng.* 27, 95 (2000)

[3] J. Madeni, S, Liu, T. Siewert, ASM International - TMS Annual Conference, Indianapolis, Conference Proceedings (2001)

[4] Westbrook, J.H. (Ed.), "*Intermetallic compounds*", John Wiley & Sons Ltd. 1967, New York, NY and Chichester.

[5] P. G. Harris and K. S. Chaggar, *Soldering Surf. Mount Technol.* 10/3, (1998), pp. 38-52

[6] Y.G. Lee and J.G. Duh, *J. Mater. Sci.: Materials in Electronics* 10 (1999), 33-43

[7] F. Bartels, J.W. Morris, Jr., G. Dalke, and W. Gust, *J. Electron. Mater.* 23, 787, (1994)

[8] S. Bader, W. Gust, and H. Heiber, *Acta Metall. Mater.* 43, 329 (1995)

[9] H.K. Kim, H.K. Liou, and K.N. Tu, *Appl. Phys. Lett.* 66, 2337 (1995)

[10] A. Hayashi, C.R. Kao, and Y.A. Chang, *Scripta Metall.* 37, 393 (1997)

[11] Jae-Yong Park, Choong-Un Kim, Ted Carper and Viswanadham Puligandla, *J. Electron. Mater.* Vol. 32, No. 11, (2003)

[12] Chi-Won Hang, Keun-Soo Kim and Katsuaki Suganuma, *J. Electron. Mater.* Vol. 32, No. 11, (2003)

[13] D.R. Flanders, E.G. Jacobs and R.F. Pinizzotto, *J. Electron. Mater.* Col. 26, No. 7, (1997)

[14] Jong-Hyun Lee and Yong-Seog Kim, *J. Electron. Mater.* Vol. 31, No. 6, (2002), pp. 576-583

[15] R.A. Gagliano, G. Ghosh, and M.E. Fine, *J. Electron. Mater.* Vol. 31, No.11, (2002), pp. 1195-1202

[16] T.H. Chuang, H.M. Wu, M.D. Cheng, S.Y. Chang, and S.F. Yen, *J. Electron. Mater.* Vol. 33, No.1, (2004), pp. 22-27

[17] P. T. Vianco, A. C. Kilgo, R. Grant, "*Intermetallic compound layer growth kinetics in non lead bearing solders*", Sandia National Laboratories, Albuquerque, NM, 1995.

[18] S. D. Yao and J. K. Shang, *IEEE Trans Complex Hybrids Manuf. Technol. B*, 19 (1996) 154.

[19] S.J. Wang and C.Y. Liu, *J. Electron. Mater.* Vol. 32, No. 11, (2003), pp. 1303-1309

[20] P. T. Vianco, P. L. Hopkins, K.L. Erikson, D. R. Frear, and R. Davidson, Design and Reliability of Solders and solder Interconnections, The Minerals, Metals and Materials Society, (1997) pp. 161-170.

[21] Kithva H. Prakash and Thirumany Srithatan, *J. Electron. Mater.* Vol. 32, No. 9, (2003), pp. 939-947.

[22] S. Choi, T.R. Bieler, J.P. Lucas and K.N. Subramanian, *J. Electron. Mater.* 28, 1209 (1999)

[22] C.B. Lee, S.J. Suh, Y.E. Shin, C.C. Shur, and S.B. Jung, Proc. 8th Symp. On Microjoining and Assembly Technology in Electronics, Yokohama, Japan: Japan Welding Society, pp. 351-356 (2002)

[23] J.W. Yoon, C.B. Lee, and S.B. Jung, *J. Electron. Mater.* Vol. 32, No. 11, (2003), pp. 1201
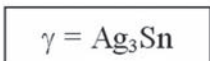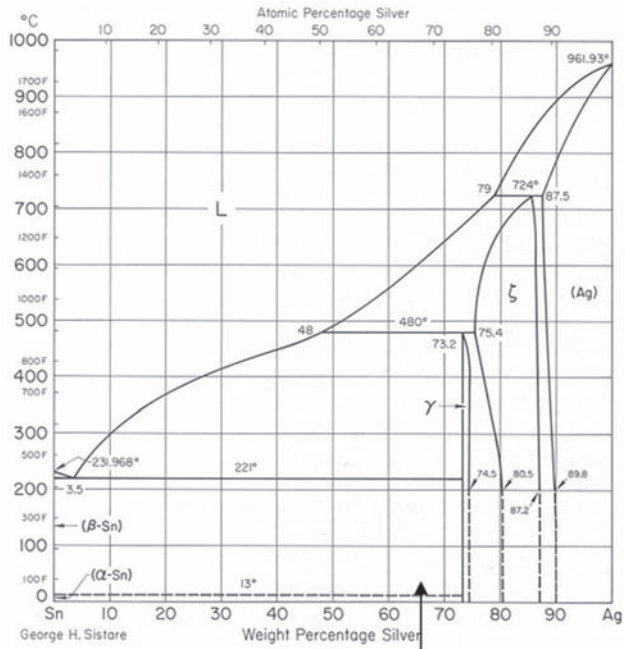
APPENDIX – A

ε = Cu₃Sn   η' = Cu₆Sn₅
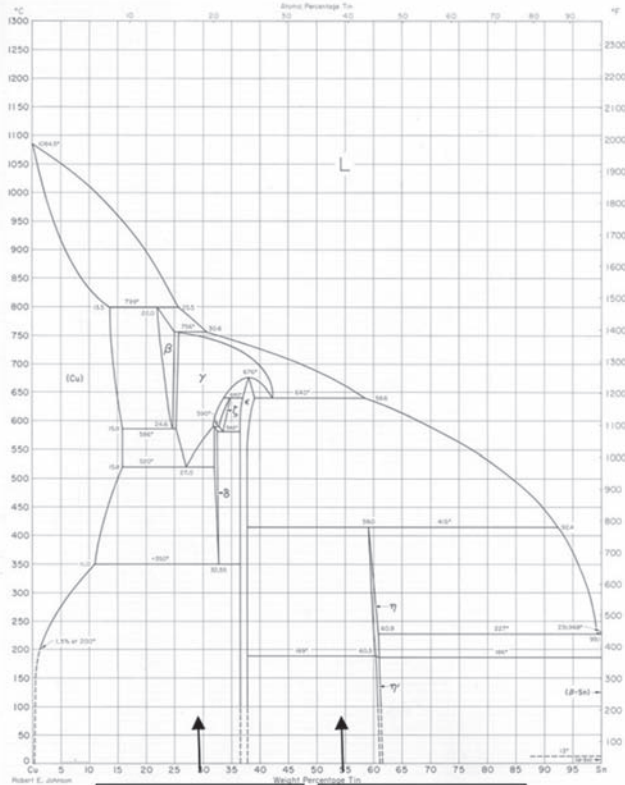
Copper-Tin equilibrium phase diagram

APPENDIX – B

γ = Ag₃Sn

Tin-Silver equilibrium phase diagram

APPENDIX – C

γ = Cu₅Zn₈

Copper-Zinc equilibrium phase diagram

Soldag. insp. São Paulo, Vol. 16, No. 1, p.086-095, Jan/Mar 2011

95